排灌机械工程学报
Journal of Drainage and Irrigation Machinery Engineering
2013 年 12 月 Dec. 2013 | 第 31 卷 第 12 期 Vol. 31 No. 12
doi:10.3969/j.issn.1674-8530.2013.12.001

Comparisons between numerical calculations and measurements in vaned diffuser of SHF impeller


Annie-Claude Bayeul-Lainé

Annie-Claude Bayeul-Lainé[1], Patrick Dupont[2], Giovanna Cavazzini[3], Patrick Cherdieu[2], Antoine Dazin[1], Gérard Bois[1], Olivier Roussette[1]
(1. Laboratoire de Mécanique de Lille(UMR CNRS 8107), Arts et Métiers ParisTech, Lille 59046, France; 2. Laboratoire de Mécanique de Lille(UMR CNRS 8107), Ecole Centrale de Lille, Villeneuve D'Ascq Cedex 59651, France; 3. Department of Industrial Engineering, University of Padova, Padova 35131, Italy)

Abstract: The paper presents analysis of the performance and the internal flow behaviour in the vaned diffuser of a radial flow pump using PIV (particle image velocimetry) and pressure probe traverses. PIV measurements have already been performed at middle height inside one diffuser channel passage for a given speed of rotation and various mass flow rates. These results have been already presented in several previous communications. New experiments have been performed using a three-hole pressure probe traverses from hub to shroud diffuser width at different radial locations between the two diffuser geometrical throats. Numerical simulations are also realized with the commercial codes Star CCM + 7.02.011 and CFX. Frozen rotor and fully unsteady calculations of the whole pump have been performed. Comparisons between numerical results, previous experimental PIV results and new probe traverses one's are presented and discussed for one mass flow rate. In this respect, a first attempt to take into account fluid leakages between the rotating and fixed part of the pump has been checked since it may affects the real flow structure inside the diffuser.

Key words: vaned diffuser; radial flow pump; unsteady flow; numerical calculations; particle image velocimetry(PIV); three-hole probe
CLC Number: S277; TH312 **Document Code**: A **Article No**: 1674-8530(2013)12-1013-08
Citation: Bayeul-Lainé A C, Dupont P, Cavazzini G, et al. Comparisons between numerical calculations and measurements in vaned diffuser of SHF impeller[J]. Journal of Drainage and Irrigation Machinery Engineering, 2013, 31(12): 1013-1021.

1 Introduction

Knowledge improvement of rotor stator interactions in radial flow pumps has already been a favourite research theme for a large number of laboratories[1-5]. Flow behaviour in radial machine is quite complex and is strongly depending on rotor stator interactions and operating conditions. A great number of rotor stator interactions analyses based on modelling activities have been realized, but experimental analyses remain scarce. Thanks to nowadays computer performances and the evolution of PIV techniques[6-7], it has been possible to measure velocity fields within the impeller and the diffuser of a radial flow pump. Tests have been performed in air with the so-called 'SHF' impeller for three kinds of diffusers: one vaneless diffuser and two differently vaned diffusers. Results obtained with the vaneless diffuser have already been presented in previous symposia and published literature[8-17].

Received date: 2013-10-21; **Publish time online**: 2013-12-17
Online Publishing: http://www.cnki.net/kcms/detail/32.1814.TH.20131217.1624.001.html
Corresponding author: **Annie-Claude Bayeul-Lainé**, Assistant professor (annie-claude.bayeul-laine@ensam.eu), research fields: turbomachinery, numerical simulation.
Note: This work has been presented in the 5th International Symposium of Fluid Machinery and Fluid Engineering, ISFMFE 2012, Korea, October 24-27, 2012.

In numerical simulation, two aspects have to be considered. The first one concerns the governing equations which are solved in the model: two kinds of numerical calculations are currently used in turbomachinery (i-frozen rotor calculations, ii-unsteady calculations). The second aspect concerns the geometrical model. Some geometrical simplifications are currently used. For example, the leakage flows are often neglected. It is obvious that a complex model(fully unsteady, with leakage flows) will be more time consuming but closer to the real physics. The aim of the paper is to test several more or less sophisticated models to evaluate their ability to predict properly the pump performance and the internal flow behaviour. To do so, numerical results are compared to experimental data[18].

The existing database has been completed by pressure probe measurements for a complete flow performance analysis. These measurements are compared to several numerical calculations in the present paper. The experimental set-up and the numerical models are presented in the first parts of the paper. The comparisons and analysis of their results (global performance as well as velocity profile) within the diffuser are then discussed.

2 Experiments

2.1 Test and apparatus

Test pump model and PIV measurements conditions have been already described[8-10] and main geometrical characteristics as well as operating conditions are given in Tab. 1. This set-up allows the existence of a "positive" leakage flow going into the gap between impeller outlet section and vaned diffuser inlet section which is specific to the experimental set-up. This is due to the fact that the pump outlet pressure corresponds to atmospheric conditions.

2.2 Three-hole probe

A three-hole probe (see Fig. 1) has been used to make hub to shroud traverses in the same planes where wall static pressures are measured. Using a specific calibration one can get total pressure, static pressure, absolute velocity and its two components in radial and tangential direction.

Tab. 1 Pump parameters

Parameter	Value
D_e/m	0.141 13
L_e/m	0.250 00
R_1/m	0.141 13
R_2/m	0.254 90
Z_i	7
h_2/m	0.040 00
Q_{ni}/($m^3 \cdot s^{-1}$)	0.337
n_i/($r \cdot min^{-1}$)	1 710
R_4/m	0.254 90
R_3/m	0.440 00
Z_d	8
h_d/m	0.040 00
Q_{nd}	$0.8Q_{ni}$
n_d/($r \cdot min^{-1}$)	1 710

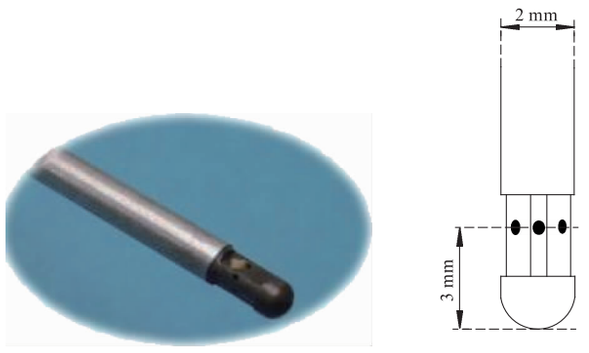

Fig. 1 Picture and sketch of the three-hole pressure probe

2.3 General flow conditions

All types of measurements have been performed for several mass flow rates. However, results presented in this paper refer mainly to one mass flow rate corresponding to the design point of the vaned diffuser $Q/Q_{ni} = 0.766$, which is different from impeller design mass flow rate $Q/Q_{ni} = 1$. This vaned diffuser design was chosen in order to allow an enlarge pump performance characteristic curve for low mass flow rates. In order to well represent the flow field, twenty-three location positions are defined as it can be seen in Fig. 2. For each location, ten axial positions are registered ($b^* = 0.125$, 0.200, 0.250, 0.375, 0.500, 0.625, 0.750, 0.875, 0.925, 0.975). The present analysis focuses only on locations 19 to 23 in the blade to blade channel of the diffuser.

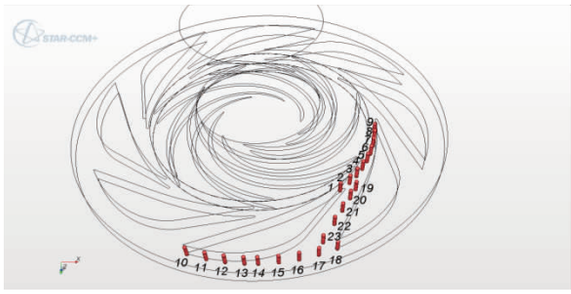

Fig. 2 Diffuser measurement locations for probe traverse and unsteady calculations

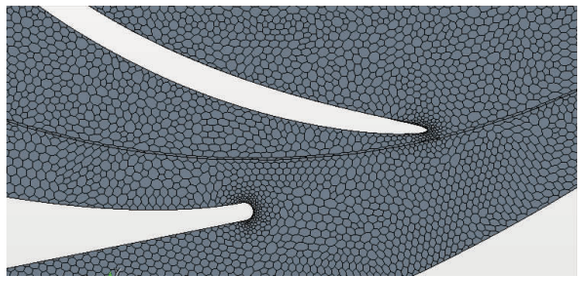

Fig. 3 Local mesh between impeller and diffuser

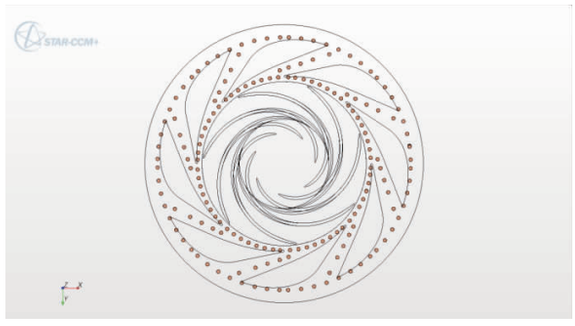

Fig. 4 Diffuser measurement locations for probe traverse and frozen rotor calculations

3 Calculations

Calculations were performed using Star CCM + code and the results are compared with already published ones obtained with CFX [8-10].

3.1 Frozen rotor calculations (Star CCM +)

Three-dimensional steady incompressible Reynolds averaged Navier-Stokes equations are solved. The SST $k-\omega$ turbulence model is used[19].

The calculation domain was divided into three zones: the inlet zone, the impeller zone and the diffuser zone.

The boundary condition at the inlet consisted of a mass flow rate ($Q_m = 0.305$ kg/s, $Q/Q_{ni} = 0.766$). The boundary condition at the outlet was the atmospheric pressure ($p = 0$ Pa). The fluid (air) was considered incompressible at a constant temperature of 20 ℃.

A polyhedral mesh with prism layers is used for all calculations (5 prism layers for a total prism layer thickness of 1 mm). The target size is 3 mm and the minimum size is 0.5 mm. The size of the grid is about 3.0×10^6 cells. A sketch of local mesh is given as shown in Fig. 3.

Line probes are plotted in the whole domain: each probe is duplicated seven times in order to obtain all parameters (pressure, total pressure, radial, tangential and axial velocity and velocity magnitude) for seven different relative positions of the diffuser comparatively to the impeller. Fig. 4 showns diffuser measurement locations for probe traverse and frozen rotor calculations. These ones are equal to $2\pi k/(1/Z_i - 1/Z_d)$ with $k = 0, 1, 2, 3, 4, 5$ and 6.

3.2 Unsteady calculations

3.2.1 Star CCM +

The unsteady calculations were realized with the same mesh. The convergence criteria are less than 1.0×10^{-4}. Maximum values of $Y+$ are around 15, and mainly below 9 in the whole computational domain as shown in Fig. 5.

A time step of 4.87×10^{-5} s, corresponding to an angular rotation of 0.5°, has been chosen.

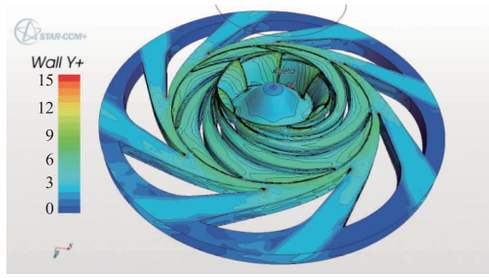

Fig. 5 $Y+$ for unsteady calculations

3.2.2 CFX

In order to investigate the influence of leakage flows, numerical results obtained using CFX are also presented. Cavazzini et al[8-10] proposed two kinds of unsteady simulations, with and without leakage flows.

As regards the simulations considering the leakage

flows, the seal systems both at the impeller inlet and outlet were modelled as shown in Fig. 6. At the labyrinth of the seal system close to the impeller inlet the mass flow rates determined from the experimental data were prescribed, assuming stochastic fluctuations of the velocities with 5% free-stream turbulence intensity. At the impeller outlet the leakage mass flow rate was controlled by the known experimental pressure in the large plenums upstream the labyrinth.

Much more details on model, mesh and numerical simulations are reported in Ref [10].

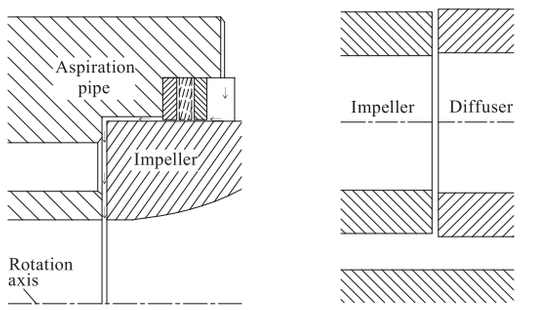

(a) Seal system at the impeller inlet (b) Seal system at the impeller outlet

Fig. 6 Seal system

4 Results and comparison

4.1 Global performances

Fig. 7 presents global results of the performance of the pump. In this figure Q^* is defined as follows:

$$Q^* = \frac{Q}{Q_n}. \tag{1}$$

Non-dimensional calculated total head is defined by equation (2) and non-dimensional isentropic head by equation(3):

$$\Psi_{tc} = \frac{dp_t}{\rho \frac{U_2^2}{2}}, \tag{2}$$

$$\Psi_{ti} = \frac{C\Omega}{Q_m \frac{U_2^2}{2}}. \tag{3}$$

Global results of total theoretical head pump are in good agreement between one dimensional approach and frozen rotor calculation. Unsteady calculation results, performed for the non-dimensional mass flow rate $Q^* = 0.766$, give the same level, as it can be seen in Fig. 7.

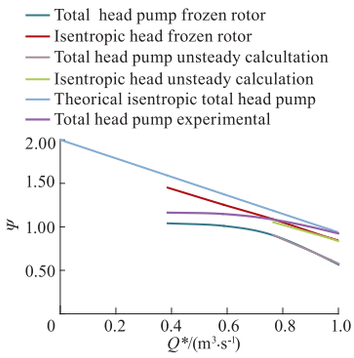

Fig. 7 Impeller non-dimensional head curve

Comparison between real total head curve obtained by calculations and experiments are also given in the same figure. One has to note that pump mass flow rates are higher than impeller mass flow rates due to "positive" leakage flow. This is the reason why the experimental head pump is higher than the numerical total pump head coefficient.

4.2 Hub-to-shroud local flow characteristics

The results obtained at location 19 have been chosen to compare frozen rotor and unsteady calculations. Numerical results are shown in Fig. 8 and Fig. 9 respectively for frozen rotor and unsteady calculations. Radial velocity distributions depend on the relative impeller blade position compared with vaned diffuser ones as shown in Fig. 8, whereas only time acts for unsteady results. Unsteady calculations give smoother hub to shroud gradients and less difference between blade to blade results.

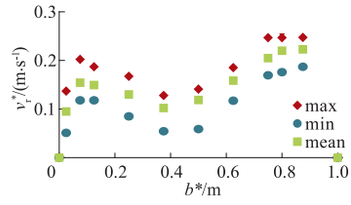

Fig. 8 Hub-to-shroud non-dimensional radial velocity in different blade to blade channels for probe 19 (frozen rotor calculation)

Local numerical results of frozen rotor calculations without leakage ("CCM + 1"), unsteady calculations without leakage (obtained from two different codes: "CCM + 2" and "CFX 1"), and unsteady calculations with leakage (obtained only from CFX [10]: "CFX 2") are presented in Fig. 10 – 13. PIV measurements ("PIV"), wall static pressure ("p_s") and three-hole

pressure probes ("probes") results are plotted on the same figures.

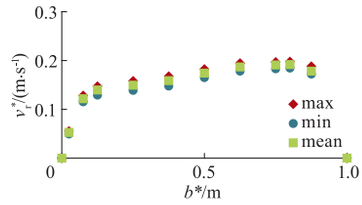

Fig. 9 Hub-to-shroud non-dimensional radial velocity in different blade to blade channels for probe 19 (unsteady calculation)

These experimental results have been performed with pump configuration with leakage. Results present radial and tangential velocities, static and total pressures distribution from hub to shroud section and for several channel locations as already shown in Fig. 2.

The influence of leakage can be easily seen when comparing numerical results obtained without and with leakage. Experimental results are in good agreement with calculations obtained with leakage. This can be mainly seen on radial velocity distribution shown in Fig. 10. These results must be more deeply analysed, in particular PIV ones; they strongly depend on impeller position and only time-averaged values are presented here. Pressure probe results are also depending on unsteady effects and this has to be taken into account for further data reduction analysis.

The influence of leakage can also be seen, looking at pressure distributions in the diffuser. Static pressure recovery is better with leakage, as shown in Fig. 13. Total pressure probe results show higher levels compared with calculations without leakage and also show that leakage effects act mainly near shroud section preventing separation in location 22 and 23.

5 Conclusions

SHF pump performance and the internal flow behaviour were predicted by calculating numercial models presented in this paper. A comparison was made between experimental and numerical simulation results. Some important conclusions have been made as follows:

1) Comparisons between numerical frozen rotor assumption and fully unsteady calculations show that global performances can be obtained with frozen rotor assumption but that local values must be analysed with unsteady results even in the vaned diffuser far from impeller outlet section.

2) Results issued from different numerical approaches and experiments coming from PIV and pressure probe have been presented and compared. The pump model configuration allows leakage to be an important parameter that has to be taken into account in order to make good comparisons between numerical simulations and experiments.

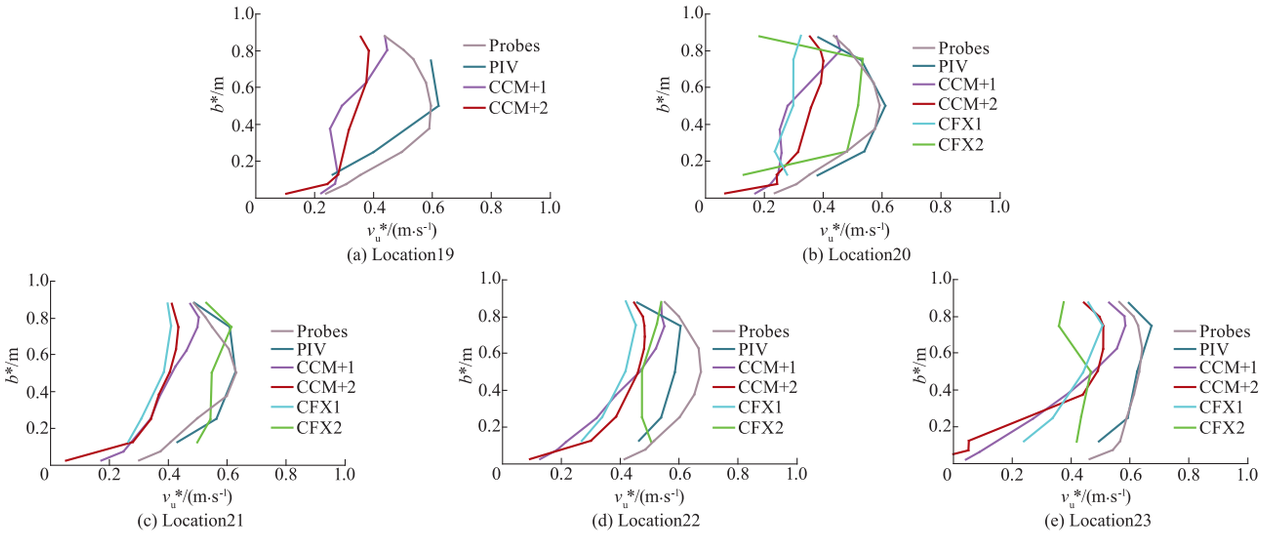

Fig. 10 Hub-to-shroud non-dimensional radial velocity v_r^* for different locations inside the diffuser channel

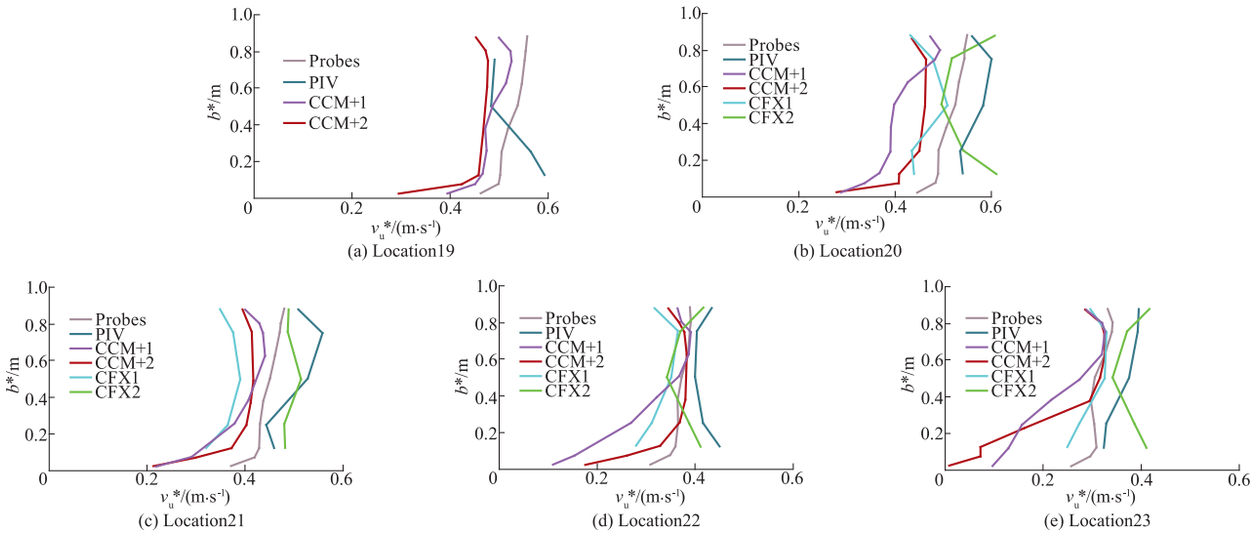

Fig. 11 Hub-to-shroud non-dimensional radial velocity v_u^* for different locations inside the diffuser channel

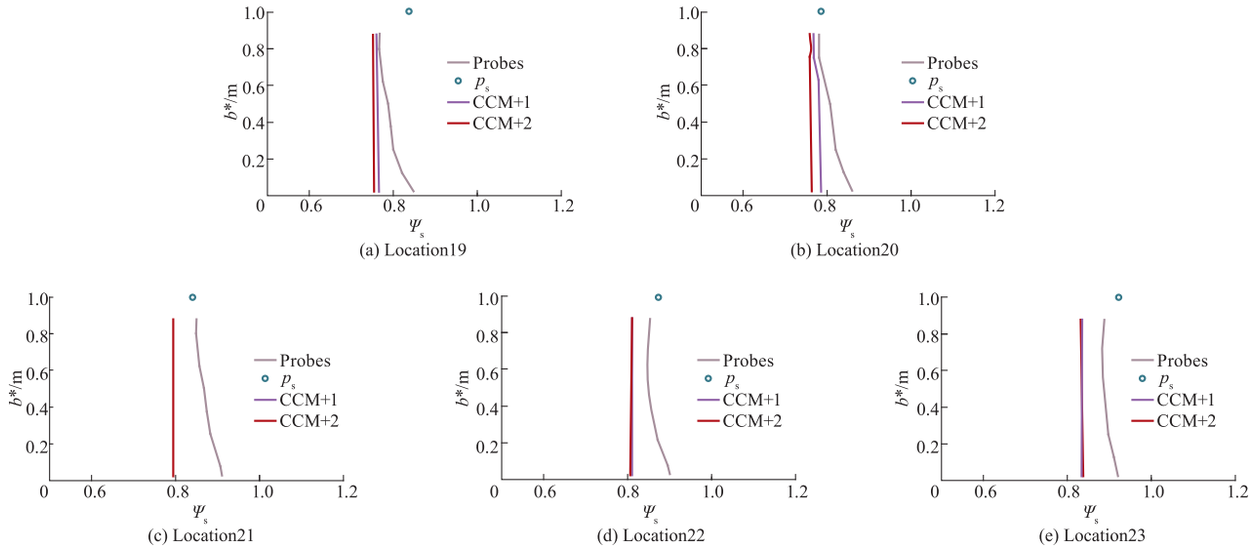

Fig. 12 Hub-to-shroud non-dimensional pressure Ψ_s for different locations inside the diffuser channel

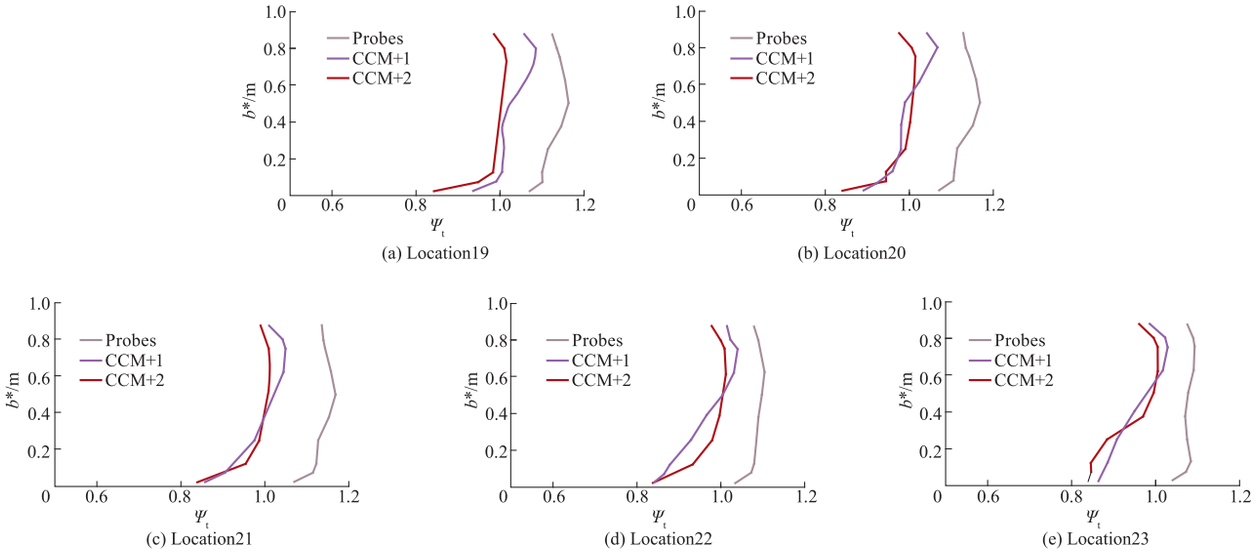

Fig. 13 Hub-to-shroud non-dimensional total pressure Ψ_t for different locations inside the diffuser channel

Acknowledgements

The authors wish to thank Region Nord-Pas de Calais and CNRS for their financial support in the frame of the CISIT program.

Nomenclature

b^*	Impeller or diffuser width	(m)
C	Impeller moment	(Nm)
D	Diameter	(m)
h	Height	(m)
H	Total pump head	(m)
n	Rotation speed	(r/min)
p	Pressure	(Pa)
p_t	Total pressure	(Pa)
Q	Volume flow rate in impeller	(m^3/s)
Q_m	Mass flow rate in impeller	(kg/s)
Q_n	Nominal volume flow rate	(m^3/s)
Q_{ni}	Impeller design flow rate	(m^3/s)
Q_{nd}	Diffuser design flow rate	(m^3/s)
R_i	Radius of section i	(m)
v_r	Radial velocity	(m/s)
$v_r^* = \frac{v_r}{U_2}$	Non-dimensional radial velocity	(–)
v_u	Tangential velocity	(m/s)
$v_u^* = \frac{v_u}{U_2}$	Non-dimensional tangential velocity	(–)
v_z	Axial velocity	(m/s)
$v_z^* = \frac{v_z}{U_2}$	Non-dimensional axial velocity	(–)
$U_2 = \Omega * R_2$	Frame velocity at impeller outlet	(m/s)
Z_i	Number of impeller blades = 7	(–)
Z_d	Number of diffuser blades = 8	(–)
ρ	Air density	(kg/m^3)
Θ	Azimuthal vane blade angle	(°)
Ω	Angular velocity	(rad/s)
ψ_{tc}	Non-dimensional total pump head	(–)
ψ_{ti}	Non-dimensional isentropic head	(–)

Index

1	Impeller inlet
2	Impeller outlet
3	Diffuser outlet
4	Diffuser inlet
c	Calculated
d	Diffuser
e	Entry duct
i	Impeller or isentropic

References

[1] Akhras A, Hajem M E, Champagne J Y, et al. The flow rate influence on the interaction of a radial pump impeller and diffuser [J]. International Journal of Rotating Machinery, 2004, 10 (4): 309 – 317.

[2] Pedersen N, Jacobsen C B. PIV investigation of the internal flow structure in a centrifugal pump impeller [C]//Proceedings of the 10th International Symposium on Applications of Laser Techniques to Fluid Mechanics, Lisbon: [s. n.], 2000: 1 – 11.

[3] El Hajem M, Morel R, Spettel F, Bois G. Etude de l'écoulement moyen en sortie de roue d'une pompe centrifuge (roue SHF) [J]. La Houille Blanche, 1998, 4: 24 – 31.

[4] Casey M V, Eisele K, Zhang Z J, et al. Flow analysis in a pump diffuser Part 1: LDA and PTV measurements of the unsteady flow [J]. ASME, Fluids Engineering Division, 1995, 229: 89 – 100.

[5] Arndt N, Acosta A J, Brennen C E, et al. Experimental investigation of rotor-stator interaction in a centrifugal pump with several diffusers [J]. Journal of Turbomachinery, 1990, 112(1): 98 – 108.

[6] Feng J J, Benra F K, Dohmen H J. Comparaison of periodic flow fields in a radial pump among CFD, PIV and LDV results [J]. International Journal of Rotating Machinery, 2009: ID 410838.

[7] Sinha M, Katz J. Quantitative visualization of the flow in a centrifugal pump with diffuser vanes— Ⅰ: On flow structures and turbulence [J]. Journal of Fluids Engineering, 1999, 122(1): 97 – 107.

[8] Cavazzini G, Dupont P, Pavesi G, et al. Analysis of unsteady flow velocity fields inside the impeller of a radial flow pump: PIV measurements and numerical calculation comparisons [C]//Proceedings of ASME-JSME-HSME Joint Fluids Engineering Conference, New York: ASME, 2011: 747 – 754.

[9] Dazin A, Cavazzini G, Pavesi G, et al. High-speed stereoscopic PIV study of rotating instabilities in a radial vaneless diffuser [J]. Experiments in Fluids, 2011, 51(1): 83 – 93.

[10] Cavazzini G, Pavesi G, Ardizzon G, et al. Analysis of the rotor-stator interaction in a radial flow pump [J]. La Houille Blanche, 2009(5): 141 – 151.

[11] Dazin A, Coutier-Delgosha O, Dupont P, et al. Rotating instability in the vaneless diffuser of a radial flow pump [J]. Journal of Thermal Science, 2008, 17(4): 368 – 374.

[12] Wuibaut G, Bois G, El Hajem M, et al. Optical PIV and LDV comparisons of internal flow investigations in SHF impeller [J]. International Journal of Rotating Machinery, 2006:1 - 9.

[13] Wuibaut G, Bois G, Dupont P, et al. Rotor stator interactions in a vaned diffuser of a radial flow pump for different flow rates using PIV measurement technique [C]//proceedings of 9th International Symposium on Transport Phenomena and Dynamics of Rotating Machinery ISROMAC 9, Hawaii, USA, 2002:FD - ABS - 018.

[14] Wuibaut G, Bois G, Dupont P, et al. PIV Measurements in the impeller and the vaneless diffuser of a radial flow pump in design and off design operating conditions [J]. Journal of Fluids Engineering, 2002, 124(3): 791 - 797.

[15] Wuibaut G, Dupont P, Bois G, Analysis of flow velocities within the impeller and the vaneless diffuser of a radial flow pump [J]. Journal of Power and Energy, 2001, 215(6): 801 - 808.

[16] Wuibaut G, Dupont, P, Bois G, et al. Application de la vélocimétrie par images de particules à la mesure simultanée de champs d'écoulements dans la roue et le diffuseur d'une pompe centrifuge [J]. La Houille Blanche, 2001(2): 75 - 80.

[17] Wuibaut G, Dupont P, Caignaert G, et al. Experimental analysis of velocities in the outlet part of a radial flow pump impeller and the vaneless diffuser using particle image velocimetry [C]//Proceedings of the 20th IAHR Symposium on Hydraulic Machinery and System, Charlotte, USA:[s. n.],2000.

[18] Menter F R. Two-equation eddy-viscosity turbulence models for engineering applications [J]. AIAA Journal, 1999, 32(8): 1598 - 1605.

[19] Petit O, Nilsson H. Numerical investigation of unsteady flow in a centrifugal pump with a vaned diffuser [J]. International Journal of Rotating Machinery, 2013: ID 961580.

(特约编辑 王应宽 责任编辑 盛杰)

沉痛哀悼全国农业水土工程专业委员会副主任彭世彰教授!

中国共产党党员,全国农业水土工程专业委员会副主任,河海大学教授、博士生导师彭世彰同志在讲座过程中突发疾病,经抢救无效于2013年12月15日18时50分不幸在南京逝世,享年54岁.

彭世彰教授生于1959年10月20日,上海市人,1985年5月加入中国共产党. 先后获河海大学学士、硕士和博士学位. 1999年11月晋升教授,2003年6月被聘为博士生导师. 先后担任河海大学水利水电工程学院副院长、河海大学科学研究院副院长、水文水资源与水利工程科学国家重点实验室常务副主任、水文水资源与水利工程科学国家重点实验室主任等职务.

彭世彰教授一生致力于水资源高效利用模式、节水灌溉理论、灌溉排水新技术及其农田生态效应等方向的研究和教学工作. 他提出了以"水稻控制灌溉"为代表的节水灌溉新理论,先后在全国近10个省市区的水稻灌区推广应用,取得了显著的经济效益和社会效益;负责和承担了国家973计划、国家863计划、国家科技攻关计划重点项目、国家科技支撑计划项目、国家自然科学基金重点项目和面上项目以及部省级重点重大科研项目等50余项;发表了学术论文220余篇,其中SCI、EI检索论文79篇;因其在农业节水领域的杰出贡献,作为全球唯一获奖者获得2012年ICID国际节水技术奖;获国家科学技术进步奖二等奖2项、三等奖1项,省部级科学技术进步奖一等奖4项、二等奖2项、三等奖5项;博士学位论文被评为"全国百篇优秀博士论文";主编和参编著作教材10部及全国规范2部;被评为江苏省跨世纪学科带头人、江苏省"333高层次人才工程"中青年科技领军人才;曾荣获全国"五一"劳动奖章、江苏省"五一"劳动奖章、江苏省优秀青年骨干教师、水利部优秀教师等荣誉称号;享受国务院政府特殊津贴.

彭世彰教授多年来一直关心和支持本刊的发展. 彭世彰教授的因公殉职,是我国农田水利界的重大损失. 他的英年早逝,使我们失去了一位优秀的党员、敬业的良师. 他勇于开拓、忠于职守、严格要求的敬业精神和为人正直、光明磊落、不计名利的高尚品格将永远激励着我们.

(本刊编辑部)